THE USE OF THE THEMATIC MAPPER FOR COASTAL WATER ANALYSIS

Commission of the European Communities
Joint Research Centre - Ispra Establishment
Physics Division
21020 Ispra (Va)
Italy
Commission number 7

1. INTRODUCTION

The potential of the land-focused Thematic Mapper (Engel, 1983) for marine applications has recently been examined by several investigators (Lathrop and Lillesand, 1986; Rimmer et al., 1987; Tassan, 1986,1987) with generally positive conclusions. The aim of this paper is to present an outline of the various problems encountered in the use of the Thematic Mapper for monitoring water quality, as well as of some aspects of the data interpretation procedures tested by the author. The performance of the Coastal Zone Color Scanner (Hovis, 1981) was taken as a reference standard. Table 1 presents a list of CZCS and TM performance parameters relevant to water sensing.

The water quality parameters usually retrieved from remote measurements of water colour are the chlorophyll-like pigment (briefly: chlorophyll) concentration and the total suspended sediment (briefly: sediment) concentration in the euphotic layer. The CZCS data are most frequently used in chlorophyll (C, mg/m^3) and sediment (S, g/m^3) retrieval algorithms of the form:

$$\log(C) = A' + B' \log(R1/R3)$$

$$\log(C) = A'' + B'' \log(R2/R3)$$

$$\log(S) = A''' + B''' \log(R3)$$

where R1 is the irradiance reflectance for band 1, etc., and A,B are numerical constants. For analogy, Tassan (1986) proposed TM retrieval algorithms of the type:

$$\log(C) = a' + b' \log(R1/R2)$$

$$\log(S) = a'' + b'' \log(R2)$$

with reference to the TM band numbers.

Inspection of Table 1 allows one to anticipate that the relatively low gain and signal-to-noise values of the Thematic Mapper are likely to cause significant problems in marine applications. These and other aspects of TM radiometry are presented elsewhere (Tassan, 1988a). It is only mentioned here that, provided appropriate procedures are used (image destriping, pixel clustering, moving average, etc.), the quality of the information which can be obtained from the analysis of TM data is not substantially lower than that yielded by the interpretation of CZCS data.

The aspects of TM data analysis which are considered in some detail in the following paragraphs are those related to: atmospheric correction, retrieval algorithm sensitivity, masking effect of sun-glitter.

2. ATMOSPHERIC CORRECTION

2.1 General algorithm

The atmospheric correction is a fundamental data interpretation level since up to 90% of the remotely measured radiance may be originated in the atmosphere itself due to molecular and aerosol scattering. According to the procedure, originally suggested by Gordon (1978) for the interpretation of CZCS data, the atmospheric correction to the remotely measured radiance $L(\lambda)$ yields the water upwelling radiance $L_W(\lambda)$ by the expression:

$$L_W(\lambda) = \frac{1}{T(\lambda)} \left\{ L(\lambda) - L_R(\lambda) - \varepsilon(\lambda,\lambda_o) \left[L(\lambda_o) - L_R(\lambda_o) - L_W(\lambda_o) T(\lambda_o) \right] \right\} \quad (1)$$

with: T = diffuse transmittance of the atmosphere; L_R = Rayleigh path-radiance, i.e. radiance scattered by the air molecules into the sensor; λ = central wavelength of the sensor band; $\varepsilon(\lambda,\lambda_o) = L_A(\lambda)/L_A(\lambda_o)$, where L_A is the aerosol path-radiance; λ_o = 670 nm (CZCS band 4). $\varepsilon(\lambda,670)$ can be evaluated from remotely measured data pertaining to "clear water" areas (i.e. with $C \leq 0.2$ mg/m^3). The original correction procedure was based on the approximation that $L_W(670)$ is negligible. This constraint has been successively removed, based on correlations among the L_W's in the four bands, through an iterative computation (Smith and Wilson, 1981; Gordon et al., 1983).

With respect to its use in Eq.(1), the radiance measured by TM band 3 (central wavelength 660 nm, bandwidth 67 nm) is substantially equivalent to the radiance measured by CZCS band 4 (λ = 670 nm, $\Delta\lambda$ = 20 nm). It follows that the above atmospheric correction method, developed for the CZCS, can, in principle, be applied to the analysis of TM data. In fact, TM band 4 (λ = 838 nm) radiance can also be used in Eq.(1), offering the two-fold advantage that (1) band 3 radiance becomes available as retrieval variable, (2) $L_W(838)$ in the right-hand side of Eq.(1) is mostly negligible. On the other hand, this band includes the 0.8 μ water vapour absorption level (Kondratyev, 1969), which may yield a significant error source.

Computation of the reduction in the band 4 radiance caused by water vapour absorption requires as input the vertical and horizontal distributions of water vapour mass, which are rapidly changing with time and generally not known with sufficient precision. In fact, neglecting H_2O absorption increases $\varepsilon(\lambda,838)$ but decreases $L(838)$ in the atmospheric correction algorithm, the two opposite effects tending to balance out. A test performed in the northern Adriatic Sea (Tassan, 1987), under the assumption that the water vapour mass is horizontally uniform with absolute value corresponding to a mid-latitude Winter atmosphere (2.5 g/cm^2), yielded:

$$C''/C' = 1.015 + .01C' \quad \text{for} \quad .05 < C(\text{mg/m}^3) < 15,$$

$$S''/S' = .959 - .001S' \quad \text{for} \quad .5 < S(\text{g/m}^3) < 10,$$

where the single and double primes indicate correction of band 4 data for water absorption applied and neglected, respectively (computation according to Tanrè et al., 1986).

The situation is not as favourable in the presence of significant variations of H_2O content over the TM scene. Assuming a variation in H_2O concentration equal to the maximum spread observed in the northern Adriatic basin by Dalu (1986), i.e. $\pm$ 0.5 g/cm^2, the corresponding retrieval error was computed to be about $\pm$ 30% for $0.1 < C(\text{mg/m}^3) < 10$ and $\pm$ 20% for $0.5 < S(\text{g/m}^3) < 10$.

Altogether, the water vapour absorption does not seem to represent a critical limitation to the use of TM band 4 data in the atmospheric correction algorithm, even if particular cases of very heterogeneous H_2O distributions may pose problems.

Other drawbacks of the use of TM band 4 data, instead of band 3 data, in the atmospheric correction algorithm, are: the lower band count rate and signal-to-noise ratio, the heavier striping and the large value of the factor $\varepsilon(\lambda,\lambda_o)$ in Eq.(1). The first two error sources are reduced to an acceptable level by the routine set-up for the radiometric calibration of TM data (Tassan, 1987). Striping of TM band 4 data is much more severe than that of band 3 data. Of the three causes of striping (droop, level shift, hysteresis, see Mezeler et al., 1985), the latter, which produces a signal undershoot at the sharp transition from high to low radiance values in the scan direction, is the most difficult to be corrected for, since it depends on the coastline morphology. For instance, a particularly complex striping pattern is generated in the Gulf of Naples (Andreoli et al., 1988) due to the superposition of contributions from neighbouring land-sea interfaces.

A statistical filter (Mehl et al., 1980), combined with some smoothing obtained by running averages, yielded satisfactory results even in the above area. A cumbersome, but more effective, destriping procedure based on the analysis of the shutter obscuration time at the end of each TM scan, is being implemented. Thus, striping does not prevent the use of TM band 4 data for the calibration of the atmospheric correction algorithm, but requires an accurate preliminary filtering.

The observed values $\varepsilon(\lambda_1,\lambda_4)$ are considerably higher than the corresponding $\varepsilon(\lambda_1,\lambda_3)$'s (for instance in the TM scene of the Gulf of Naples of July 6, 1987, $\varepsilon(\lambda_1,\lambda_4) = 3.29$ vs $\varepsilon(\lambda_1,\lambda_3) = 1.51$). Thus, the magnification of any error affecting the term of Eq.(1) within square brackets is larger when these contain band 4 data. An important error source magnified by the ε factor is that associated to sun-glitter.

Finally, close to land covered by green vegetation, band 4 radiance values measured over sea pixels are increased by the contribution from the much higher band radiance reflected by neighbouring land, which is scattered into the sensor field of view by the atmosphere. In the Gulf of Naples, the above increase reached 30% of the correct sea value just off the coastline, decaying to a negligible magnitude in about one mile. This effect can be corrected for either by theoretical computation (Tanrè et al., 1986) or directly from the analysis of the TM image replacing the anomalous band 4 data with the correct sea values nearby. The above information may serve as a guideline for the choice of the TM band data to be used in the atmospheric correction algorithm expressed by Eq.(1).

Both band 3 and band 4 data have been used to evaluate the atmospheric correction to TM data of the northern basin of the Adriatic Sea (Tassan, 1987). Except for some details close to the coast, the maps of chlorophyll and sediment concentrations obtained appeared very similar. A systematic comparison, carried out for 50 pixels representative of the C,S variation range observed for the TM scene of October 15, 1984, yielded:

$$C_3/C_4 = 1.12 + .005\ C_4 \qquad \sigma_{x,y} = .35 \qquad .1 < C(mg/m^3) < 15$$

$$S_3/S_4 = 1.10 + .016\ S_4 \qquad \sigma_{x,y} = .32 \qquad .3 < S(g/m^3) < 15$$

i.e.: a minor ($\sim$ 10%) systematic difference between the two sets of results, almost constant over the considered concentration ranges (C_3 = chlorophyll content retrieved if band 3 data are used in Eq.(1), etc.).

2.2 Simplified algorithm

The algorithm of Eq.(1) accounts for horizontal variations of the aerosol mass over the scene, relying only on the assumption that the aerosol phase function remains constant. Over small-size scenes of coastal zones the horizontal distribution of the aerosol mass is frequently uniform. In this case the atmospheric correction algorithm can be considerably simplified. In fact, in the synthetic expression:

$$L(\lambda) = L_R(\lambda) + L_A(\lambda) + L_w(\lambda) \cdot T(\lambda) \qquad (2)$$

the terms $L_R(\lambda)$,$T(\lambda)$ are calculated theoretically (e.g. Tanrè et al., 1986), $L_A(\lambda)$ is inferred from the analysis of "clear water" pixels, where the values of $L_w(\lambda)$ are known (Gordon et al., 1983). Thus, after some correction to $L_R(\lambda)$ and $L_A(\lambda)$ associated to the variable scanner zenith angle, for each pixel:

$$L_w(\lambda) = \frac{1}{T(\lambda)} [L(\lambda) - L_R(\lambda) - L_A(\lambda)] \qquad (3)$$

Whenever applicable, this simplified algorithm presents a number of advantages over the general atmospheric correction model expressed by Eq.(1), such as: lower numerical error, lower sensitivity to image striping and variable sun-glitter, reduced computational labour. Both the general and the simplified schemes of atmospheric correction were satisfactorily applied to TM data regarding the Gulf of Naples (Andreoli et al., 1988).

2.3 Variation of the atmospheric correction on the scan direction

The coupling of the LANDSAT orbit (heading 10.87°, equator crossing time 9.30 hrs) with the TM swath (± 7.5° from nadir normal to the flight direction) induces a significant variation in $L_R(\lambda)$ and $L_A(\lambda)$ along the scan direction. This is due to the circumstance that the sensor scan and the sun lie almost on the same azimuthal plane, so that even the minor ± 7.5° swath causes an appreciable change in the angle ψ between sun and sensor view directions and, thus, on the phase function of molecular and aerosol scattering. For instance, in the area of the Gulf of Naples, on July 6, 1987, with sun azimuth and zenith angles φ^o = 116.07, θ^o = 30.6 and scan azimuth φ = 100.87, the extremes of the TM swath correspond to ψ = 142.10 (East) and ψ = 156.55 (West).

The effect of this variation of ψ on the remotely measured radiance term associated to molecular scattering is easily computed (Sturm, 1984), the Rayleigh phase function being:

$$f_R(\psi) = \frac{3}{16 \cdot \pi} (1 + \cos^2(\psi)) \qquad (4)$$

It turns out that this term increases by 13.6% from East to West. Considering that the nadir value of $L_R(485)$ computed for the scene of the Gulf of Naples of July 6, 1987, was 3.47 mW/(cm^2·sr·μ), while the observed values of $L_w(485)$ ranged .07 ÷ .7 mW/(cm^2·sr·μ), it is evident that the space variation of the Rayleigh path radiance must be accurately accounted for in the evaluation of the atmospheric correction by either Eq.(1) or Eq.(3). This entrains some computational labour, but does not represent a significant error source.

On the contrary, the evaluation of the effect of the variation in the angle

ψ on the remotely measured radiance term due to aerosol scattering is rather uncertain. The most frequently used model for the aerosol phase function is the two-term Henyey-Greenstein function:

$$f_A(\psi) = \frac{(1-g_1^2)\cdot\alpha}{(1+g_1^2-2g_1\cos\psi)^{3/2}} + \frac{(1-g_2^2)(1-\alpha)}{(1+g_2^2+2g_2\cos\psi)^{3/2}} \qquad (5)$$

where g_1, g_2, α are numerical constants whose value depends on the aerosol type (Tassan et al., 1979). Since the aerosol type present in the area covered by the TM scene is generally not known with sufficient accuracy, one must use estimates of g_1, g_2 and α, which may yield a significant uncertainty in the $f_A(\psi)$ value computed by Eq.(5).

Fortunately, the magnitude of $L_A(\lambda)$ is usually considerably less than that of $L_R(\lambda)$, so that the impact of the error in $L_A(\lambda)$ on the atmospheric correction is also lower. For instance, in the considered July 6 scene, even with a rather turbid atmosphere characterized by a horizontal visibility around 8 km, the value of $L_A(485)$ was about half that of $L_R(485)$.

3. SENSITIVITY OF THE RETRIEVAL ALGORITHMS

The currently used retrieval algorithms are in the form $\log y = A+B \log x$, where y,x are the retrieved quantity and the retrieval variable, respectively, and A,B are numerical constants. A fundamental requirement is the sensitivity of the retrieval variable to the retrieved quantity, i.e. its ability to detect small variations in this quantity. The sensitivity is a function of the wavelength and width of the sensor bands. For algorithms of the type $\log y = A+B \log x$ one obtains $dy/y = B\, dx/x$ by elementary differentiation. It follows that 1/B can be taken as a measure of the previously defined sensitivity of the retrieval variable.

Numerical values of the constants A,B for CZCS and TM algorithms used to retrieve chlorophyll and sediment concentrations in different water types have been determined both by theoretical computation and by in-situ measurements. The results obtained for the northern basin of the Adriatic Sea (Tassan and Sturm, 1986; Tassan, 1987) are presented below:

Sensor	Retrieved parameter	Retrieval variable	$B_{theor.}$	$B_{exp.}$
CZCS	chlorophyll	R443/R550	-1.79	-2.19±.13
	sediment	R550	1.82	1.66±.14
TM	chlorophyll	R485/R570	-2.43	-2.73±.19
	sediment	R570	1.79	1.70±.14

One remarks that
- the theoretical and experimental values for the algorithm sensitivities are generally in good agreement;
- the sensitivity of the TM algorithm for chlorophyll retrieval is not much lower than that of the CZCS algorithm;
- the TM and CZCS sensitivities for sedimental retrieval are alike.

These trends were confirmed by the results obtained for other water types. For instance, a set of in-situ measurements carried out in the Gulf of Naples yielded (Andreoli et al., 1988):

$$\text{CZCS:} \quad \log(C) = (-.02\pm.05) + (-1.64\pm.13)\ \log(R443/R550) \qquad (6)$$

$$\text{TM:} \quad \log(C) = (\ .23\pm.04) + (-2.52\pm.14)\ \log(R485/R570)$$

The statistical quality indices of the CZCS and TM algorithms are remarkably similar.

4. SUN-GLITTER

Sun-glitter is caused by direct sun radiation reflected by the wave facets into the sensor field of view. It adds to the remotely measured radiance a term, whose magnitude critically depends on wind speed and sun elevation. CZCS was provided with a device to tilt it away from the sun so as to avoid sun-glitter in all circumstances. TM scans $\pm$ 7.5° from the nadir and, thus, is affected by sun-glitter. The circumstance that the TM scan plane and the sun azimuth plane are almost coincident introduces a space dependence in the remotely measured sun-glitter, namely an increase along the scan direction from West to East, which significantly complicates the situation.

The sun-glitter variation along the TM swath may be relevant. The generally used model for sun-glitter is that proposed by Cox and Munk (1955) for steady-state conditions (wind and waves in equilibrium, no reflection from the coastline, infinite depth of the sea). Figure 1 presents a family of curves of sun-glitter vs wind speed computed by the above model for scan angles from -7° to +7° by 1° intervals (TM band 1, Gulf of Naples, time of LANDSAT 5 pass on June 21, horizontal visibility 10 km). Figures 2 and 3 show the same family of curves computed for August 21 and October 21. Considering that typical Summer values for the water upwelling radiance of TM band 1 in the same area range from 1 to .05 mW/(cm^2·sr·μ), it is evident that for a time interval of about three months centered on the Summer solstice, sun-glitter may represent a very important error source.

In steady-state conditions, with uniform wind over the analyzed TM scene, the use of the atmospheric correction algorithm expressed by Eq.(1) can yield some compensation of opposite effects, provided the "clear water" pixels data employed to evaluate $\varepsilon(\lambda,\lambda_o)$ and the pixels to which the algorithm is applied, are seen with about the same scan angle. This procedure can give satisfactory results. For instance, a computation performed for the northern Adriatic Sea for June 21 showed that neglecting sun-glitter radiance in the assessment of the atmospheric correction causes chlorophyll retrieval errors lower than 10%, provided the wind speed is less than 6 m/s (Tassan, 1987).

In reality, the wind speed and direction may be unevenly distributed over the TM scene, especially in coastal waters with complex coastline morphology and high reliefs. The detailed distribution of the wind vector is usually unknown. In this case, performing the atmospheric correction by Eq.(1) may induce large errors: the above numerical exercise yielded chlorophyll retrieval errors up to 50% when the 6 m/s wind varied by $\pm$ 1 m/s. In addition, in these waters the steady-state model of Cox and Munk is likely to fail to give valid results.

In the presence of moderate sun-glitter, the simplified atmospheric correction algorithm expressed by Eq.(3) may still be effective, being less sensitive to wind variation. Larger sun-glitter may prevent a meaningful interpretation of TM data.

A method for the evaluation of the sun-glitter contribution to the TM band radiance values, operating pixel by pixel, has been set up and is now being implemented (Tassan, 1988b). The method, which uses TM bands 4 and 5 data, is based on the generally valid assumption that these bands do not measure any significant water upwelling radiance.

5. SUPPORT BY IN-SITU MEASUREMENTS

The data interpretation schemes presented in the previous sections do not make use of in-situ measurements, except for the determination of the retrieval algorithms.

In fact, in small water bodies such as the coastal areas where TM data can yield useful information, a number of in-situ measurements centered on the time of the LANDSAT pass can often be carried out in a relatively simple way and with limited effort. If this is the case, even a small set of experiments, carefully planned, represents an important aid to the remote data analysis, providing a benchmark for calibration and validation of the results.

If a larger set of experimental stations is available, the remote data, corrected for the atmospheric effects, can be directly correlated to the chlorophyll and sediment contents measured in-situ, yielding retrieval algorithms which are then applied to the entire scene. The correlation can also be established without applying the atmospheric correction, relying on the assumption that the aerosol load is uniform over the scene. In particular cases this direct approach may yield more reliable and accurate information, provided the variability of the molecular and aerosol path-light over the scene is taken into proper account.

6. CONCLUSION

Provided procedures taylored to the specific features of this sensor are used, the interpretation of TM data appears to be capable to yield information on water quality parameters (i.e. chlorophyll and sediment concentrations) of acceptable standard. Among the tested error sources, sun-glitter seems to cause the greatest concern. Around the Summer solstice, depending on latitude, sun-glitter may represent a real limitation to the marine use of the Thematic Mapper, unless adequate corrections are applied.

The low repetition rate (one pass every 16 days) and the modest swath (188 km) prevent the use of the Thematic Mapper for the investigation of events developing within short times, as well as for large-scale identification of the phenomena. Within these limits the Thematic Mapper may prove to be effective in the analysis of coastal waters, around important localized water pollution sources, such as large urban and industrial districts, river outlets, etc.

REFERENCES

ANDREOLI G. et al., 1988, "Sea truth project", a joint research effort to validate a procedure using Thematic Mapper data to monitor the quality of coastal waters. Proc. of the 8th EARSeL Symposium, Capri, Italy (in press).

COX C. and MUNK W., 1955, "Some problems in optical oceanography", J. of Marine Research, 14, 63.

DALU G., 1986, "Satellite remote sensing of atmospheric water vapour", Int. J. of Remote Sensing, 7, 1089-1097.

ENGEL J.L., 1983, "The Thematic Mapper - instrument overview and preliminary on-orbit results", Proc. of the Soc. of Photo-Optical Instrumentation Engineers, Vol.430, Infrared Technology, Chap.IX, pp.424-435.

GORDON H.R., 1978, "Removal of atmospheric effects from satellite imagery of the oceans", Applied Optics, 17, 1631-1637.

GORDON H.R., CLARK D.K., BROWN J.W., BROWN O.D.,ZEVANS R.H. and BROENKOW W.W., 1983, "Phytoplankton pigment concentrations in the Middle Atlantic Bight: comparison of ship determinations and CZCS estimates", Applied Optics, 22, 20-35.

HOVIS W.A., 1981, "The NIMBUS-7 Coastal Zone Color Scanner", in: Oceanography from Space, edited by J.F.R. Gower (New York: Plenum Press), pp.215-226.

KONDRATYEV K., Ya., 1969, Radiation in the Atmosphere (New York: Academic Press).

LATHROP R.G. and LILLESAND T.M., 1986, "Use of Thematic Mapper data to assess water quality in Green Bay and Central Lake Michigan", Photogr. Eng. and Remote Sensing, 52, 5, 671-680.

MEHL W., STURM B. and MELCHIOR W., 1980, "Analyses of coastal zone scanner imagery over Mediterranean coastal waters", 14th Int. Symp. on Remote Sensing of Environment, 23-30 April, San José, Costa Rica (Ann Arbor: Environmental Research Institute of Michigan), pp.653-662.

METZLER M.D. and MALILA W.A., 1985, "Characterization and comparison of Landsat-4 and Landsat-5 Thematic Mapper data", Photogrammetric Engineering and Remote Sensing, 51, 1315-1330.

RIMMER J.C., COLLINS M.B. and PATTIARATCHI C.B., 1987, "Mapping of water quality in coastal waters using airborne Thematic Mapper data", Int. J. Remote Sensing, 8, 1, 85-102.

SMITH R.C. and WILSON W.B., 1981, "Ship and satellite bio-optical research in the California Bight", in: Oceanography from Space, edited by J.F.R. Gower (New York: Plenum Press), pp.281-294.

STURM B., 1984, "The atmospheric correction of remotely sensed data and the quantitative determination of suspended matter in marine water surface layers", in: Remote Sensing in Meteorology, Oceanography and Hydrology, edited by A.P. Cracknell (Chichester: Ellis Horwood), pp.163-197.

TANRE D., DEROO C., DAHAUT P., HERMAN M. and MORCRETTE J.J., 1986, "Effets atmosphériques en télédétection - logiciel de simulation du signal satellitaire dans le spectre solaire", Proc. of the 3rd Int. Colloquium on Spectral Signatures of Objects in Remote Sensing, Les Arcs, France, 16-20 December 1985, ESA SP-247 (Paris: European Space Agency), pp.315-319.

TASSAN S., 1986, "Evaluation of the potential of the Thematic Mapper for marine application", Proc. ESA/EARSeL Symp. on Europe from Space, Lyngby, Denmark, 25-27 June 1986.

TASSAN S., 1987,"Evaluation of the potential of the Thematic Mapper for marine application", Int. J. Remote Sensing, 8, 10, pp.1455-1487.

TASSAN S., 1988a, "Radiometric problems in the use of the Thematic Mapper for marine research", Proc. of the IGARSS '88 (to be published).

TASSAN S., 1988b, "A method to correct Thematic Mapper imagery for sun glitter", in preparation.

TASSAN S., STURM B. and DIANA E., 1979, "A sensitivity analysis for the retrieval of chlorophyll contents in the sea from remotely sensed radiances", Proc. of the 13th Int. Symp. on Remote Sensing of Environment, Ann Arbor, Michigan, USA (Ann Arbor: Environmental Research Institute of Michigan), pp.713-728.

TASSAN S. and STURM B., 1986, "Algorithms for the retrieval of chlorophyll and sediment concentration from CZCS data, applying to the Adriatic Sea", Programme Progress Report, JRC, Ispra Establishment, Italy.

AKNOWLEDGMENTS

The author is indebted to Mrs Margitta Metzner for the sun-glitter computation presented in Figs. 1 to 3.

TABLE 1 - CZCS and TM5 characteristic performance parameters relevant to water sensing

Sensor	Spectral bands and parameters[1]				Signal quantization levels	Ground resolution (m)	Swath (km)	Cycle (d)
	1	2	3	4				
CZCS	20	20	20	20	256	800	1625	6
	443	520	550	670				
	200	150	150	100				
	22-47	32-67	40-85	88-187[2]				
	0.9-1.6	2-4.8	3-4	1-4[2]				
TM	66	82	67	128	256	30	188	16
	485	570	660	838				
	50-140	60-280	50-250	35-342[3]				
	15.55	7.85	10.20	10.82				
	1.83	1.69	1.88	2.24				

[1]Line 1, bandwidth (nm); line 2, central wavelength (nm); line 3, signal-to-noise ratio; line 4, reflective band gain (counts per $mW/(cm^2 \cdot \mu m \cdot sr)$); line 5, bias (counts).

[2]For gains 1 and 4, respectively.

[3]For minimum and maximum scene radiance, respectively.

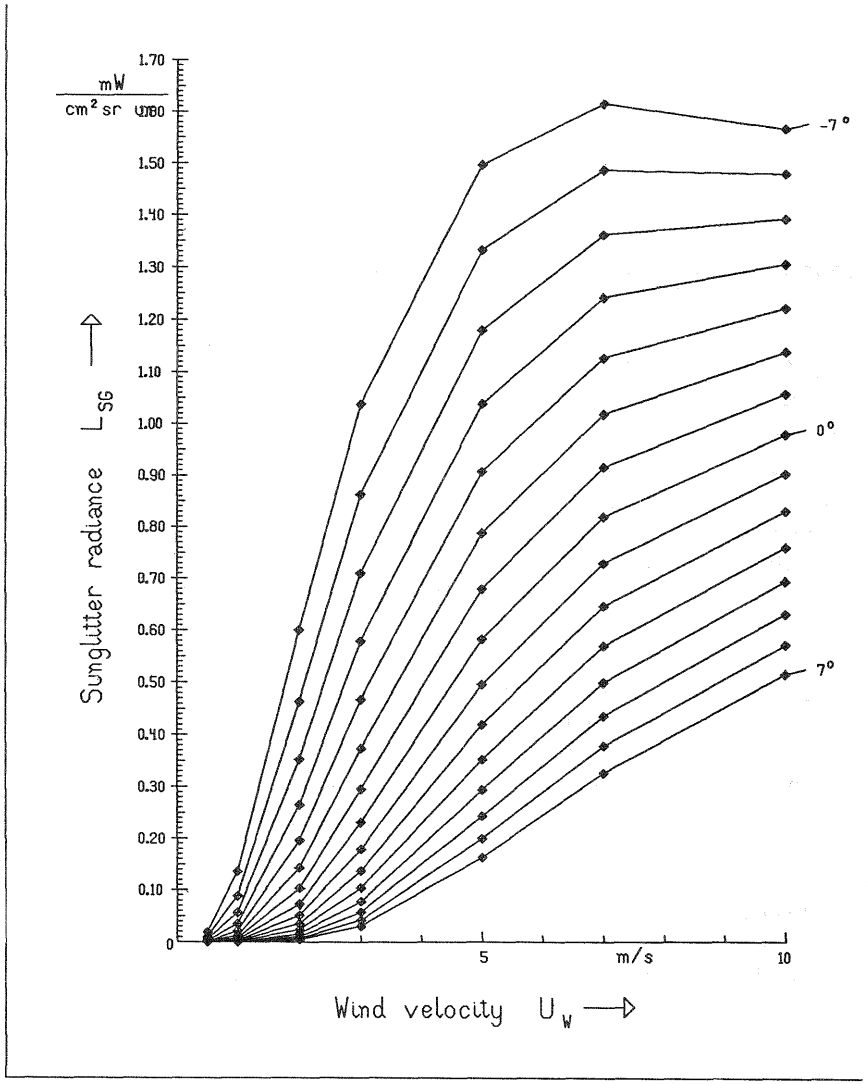

Fig. 1. Computed sun-glitter radiance as a function of scan angle (-7°,7°) and wind speed for TM band 1. Gulf of Naples, 10.00 hrs on June 21.

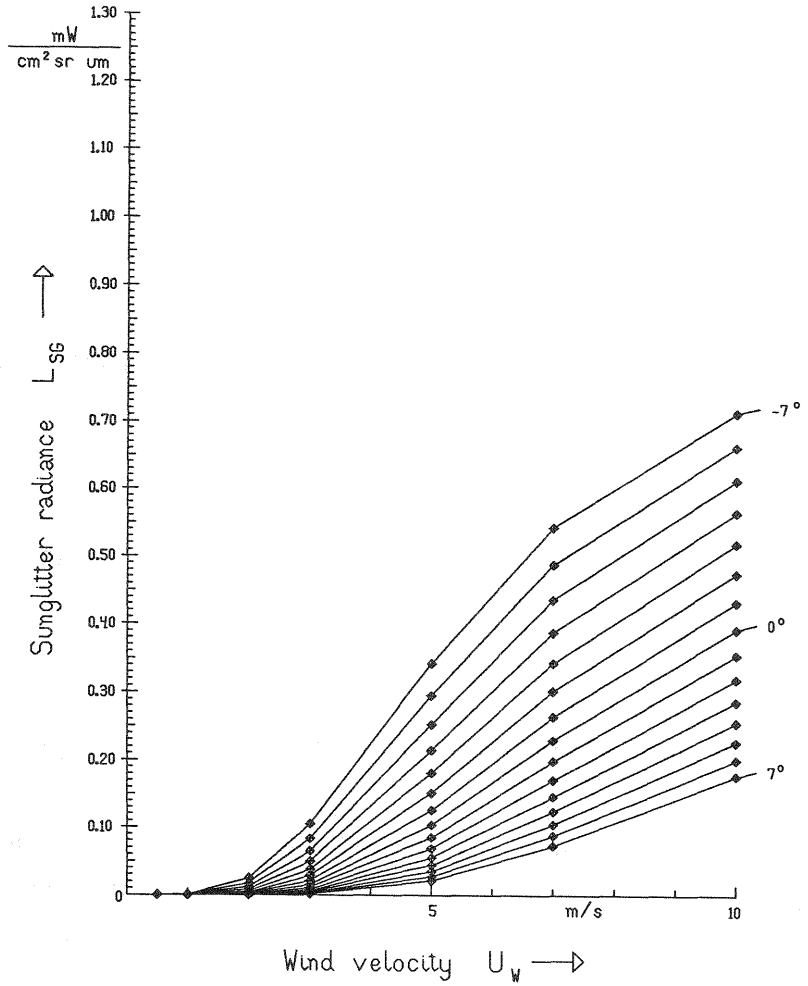

Fig. 2. Computed sun-glitter radiance as a function of scan angle (-7°,7°) and wind speed for TM band 1. Gulf of Naples, 10.00 hrs on August 21.

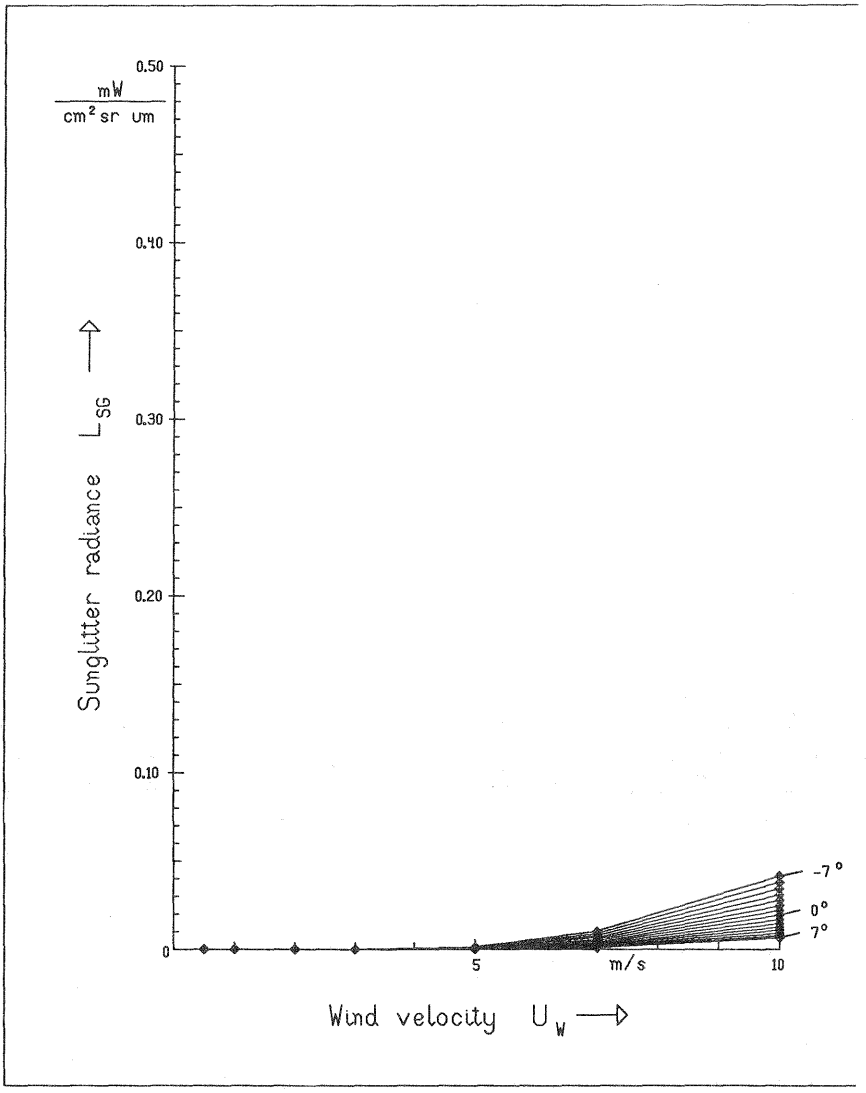

Fig. 3. Computed sun-glitter radiance as a function of scan angle ($-7^o, 7^o$) and wind speed for TM band 1. Gulf of Naples, 10.00 hrs on October 21.